



Abstract—In this study, we examined whether otolith microconstituents are deposited seasonally in a manner similar to optical annulus formation and thereby can be used to validate age interpretations. In temperate species, seasonal temperature changes drive the formation of optical annuli, and we hypothesized that they similarly caused oscillations in microconstituent deposition. Using laser ablation inductively coupled plasma mass spectrometry analysis, we tested for periodicity in the deposition of barium (Ba), calcium, copper, magnesium (Mg), manganese (Mn), phosphorus (P), strontium, and zinc in otoliths and compared that periodicity to the periodicity of the annulus zonation (optical opaque and translucent zones). For this investigation of chemical annulus periodicity, we used black sea bass (*Centropristis striata*), a species with yearly optical annulus formation that has been validated. Periodicities in elemental profiles in otoliths from black sea bass were detected by using Lomb–Scargle periodogram analyses. Optical annulus formation aligned with Mg profiles, but periodicity in annular deposition of other elements—Ba, Mn, and P—was observed only after the first optical annulus, an outcome that is indicative of ontogenetic changes in habitat (from coastal to near-shelf waters) known to occur during the juvenile life stage of this species. Certain elements, such as Mg, identified through this otolith analysis and the periodogram analyses could be applied to species for which no validated aging procedure exists.

Manuscript submitted 17 March 2023.
Manuscript accepted 29 November 2023.
Fish. Bull. 121:188–198 (2023).
Online publication date: 14 December 2023.
doi: [10.7755/FB.121.4.4](https://doi.org/10.7755/FB.121.4.4)

The views and opinions expressed or implied in this article are those of the author (or authors) and do not necessarily reflect the position of the National Marine Fisheries Service, NOAA.

Examining the periodicity of annular deposition of otolith microconstituents as a means of age validation

Benjamin Frey (contact author)¹
Vyacheslav Lyubchich¹
Michelle Zapp Sluis²

Nathaniel Miller³
David Secor¹

Email address for contact author: benalexfrey@gmail.com

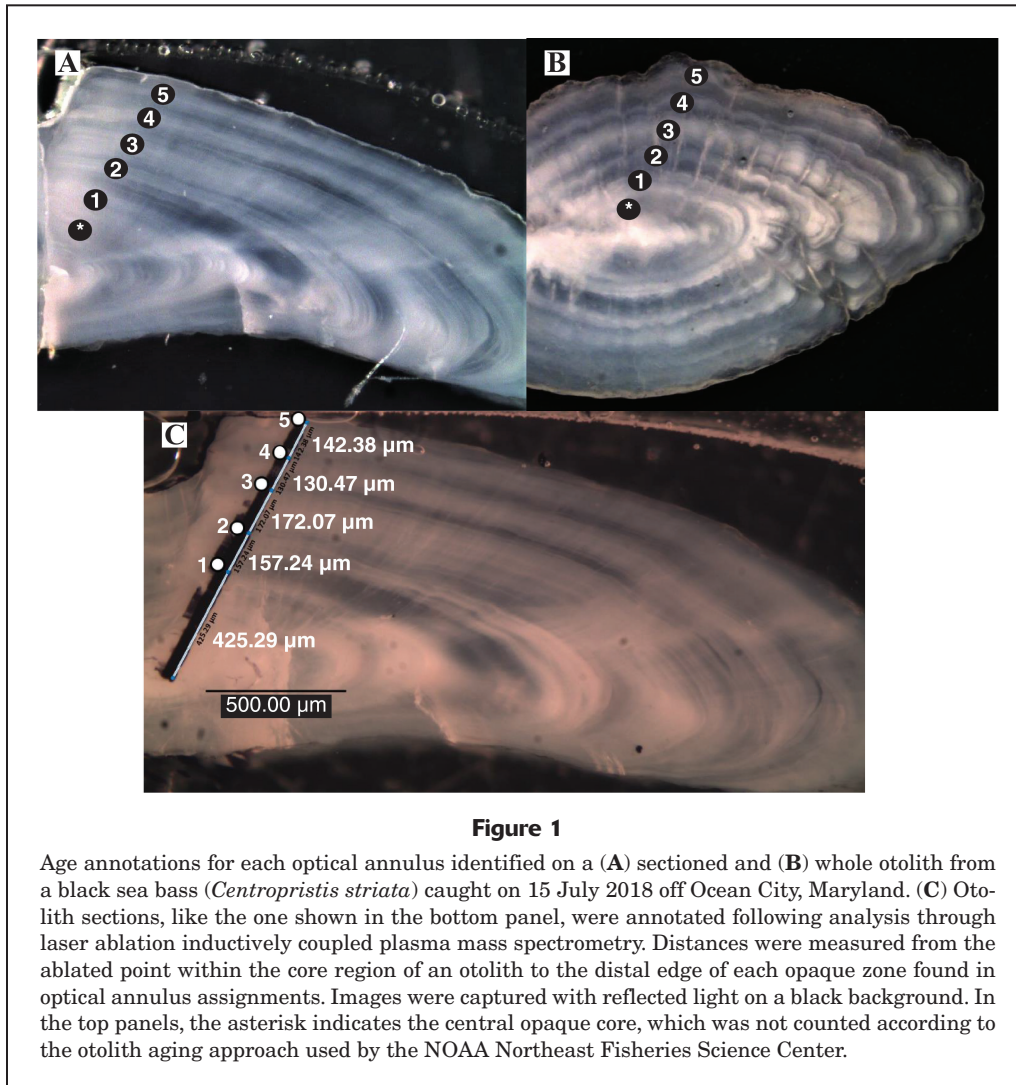
¹ Chesapeake Biological Laboratory
University of Maryland
Center for Environmental Science
146 Williams Street
Solomons, Maryland 20688

² Department of Marine Biology
Texas A&M University at Galveston
1001 Texas Clipper Road
Galveston, Texas 77553

³ Jackson School of Geosciences
The University of Texas at Austin
2305 Speedway, Stop C1100
Austin, Texas 78712-1692

The lack of validated methods for age determination directly affects many fisheries assessments and management efforts. The use of unvalidated aging techniques can affect estimation of catch at age, selectivity at age, numbers at age, maturity at age, and weight at age, and errors in estimates of these factors can contribute to major bias and errors in age-based assessments (Bradford, 1991; Wilhelm et al., 2008; Elvarsson et al., 2018). An error in aging can result in overexploitation and the eventual collapse of a stock and its associated fishery (Mills and Beamish, 1980; Chale-Matsau et al., 2001; Yule et al., 2008). Despite the importance of accurate age determinations, validation studies on annulus formation are rare for many important commercial stocks, including the majority of species harvested in waters along the Atlantic coast from Maine to South Carolina (Suppl. Table). Validation studies have been done for only slightly more than half (10 of 19; Suppl. Table) of the species routinely aged by the NOAA Northeast Fisheries Science Center.

Interpretation of optical zones (annuli) in fish hard parts is considered a direct method of aging and is the conventional approach for age determination, which is needed in age-based assessments (Casselman, 1983; Vitale et al., 2019). Hard parts are calcified structures, which include otoliths, vertebrae, opercula, fin rays, and scales. They often have patterns of seasonal zonation, which can be optically distinguished through microscopy as alternating dark and light (translucent and opaque) zones that vary in their organic concentrations (Jolivet et al., 2008) (Fig. 1). Opaque zones typically have higher protein content, are relatively narrow in comparison to translucent zones, and are interpreted as representing periods of lower seasonal growth rates such as temperate winters (Thomas, 1983; Machias et al., 1998; Zlokovitz et al., 2003). The 2 zones together constitute an annulus, but it remains the task of the investigator to determine whether each annulus forms annually and therefore whether it is valid to use the structure for determining ages of fish (Campana, 2001).



Efforts to validate age determination can be hampered by the requirement to test age interpretations on fish of known ages. The approaches used to validate the annual formation of presumed annuli in hard parts can be direct or indirect (Vitale et al., 2019). In direct validation methods, individuals are tracked over time as annular zones form over seasons and years, by using temporal reference points (markers) on hard parts (Vitale et al., 2019). In indirect validation methods, annular structures are examined in relation to changes in season, year-class strength, or size modes and include length–frequency analysis, marginal increment analysis, and microchemistry (Vitale et al., 2019).

In a promising approach for age validation, periodicity in annular deposition of microconstituents in hard parts is examined by using microchemistry. Otolith microconstituent uptake can vary seasonally and can be regarded as a “chemical calendar-clock” with time-keeping properties similar to the optical annuli on hard parts (Limburg et al., 2018). The results of the study by Hüsey et al. (2021a) reveal that the elemental composition of otoliths can vary seasonally and that these variations can be used

to validate the accuracy of otolith chemical chronologies in determining the age of fish. Siskey et al. (2016) and Brophy¹, employing periodogram analysis, have shown that the periodicity of some elements in hard parts is annual and synchronizes with the optical patterns that form annuli.

The underlying premise of microconstituent validation is that optical banding patterns (annuli) in hard parts coincide with changes in chemical composition, both of which represent seasonal changes in otolith organic content and environmental temperature. Fish that reside or migrate through coastal and shelf environments are exposed to mixtures of terrestrial, anthropogenic, and marine sources of aqueous metals and isotopes. Found in higher abundance in hard parts than calcium (Ca), the elements strontium (Sr), magnesium (Mg), manganese (Mn), and

¹ Brophy, D. (coord.). 2019. Validating age-determination [sic] of anglerfish and hake, 97 p. EASME/EMFF/2016/1.3.2.7/S12.762036. Final report. Publ. Off. Eur. Union, Luxembourg, Luxembourg. [Available from [website](#).]

barium (Ba) substitute for Ca within the crystalline lattice of aragonitic otoliths in proportion to environmental exposure but at rates modified by temperature and growth (Hüssy et al., 2021b). Trace constituents, such as phosphorus (P), cobalt (Co), copper (Cu), and zinc (Zn), are bound in the protein matrix of otoliths and it has been hypothesized that they are physiologically controlled (Hüssy et al., 2021b), albeit some evidence indicates a role for environmental exposure (Arslan and Secor, 2005). Therefore, across the elements that we considered candidates for use in age determination, the kinetics of tracer incorporation are driven variously by exposure, temperature, and physiology, the relative contribution of which remains an unsettled question (e.g., Hüssy et al., 2020).

In temperate shelf environments, concentrations of candidate elements do not vary as substantially as they would in freshwater, estuarine, and nearshore environments. In this study, we assumed that exposure to seasonally changing temperatures drives variation in microconstituent concentrations. We tested this assumption by comparing known seasonal patterns of optical annulus zonation with those of microconstituent zonation in otoliths.

To evaluate chemical annulus periodicity, it's important to test a model species for which age determination has been validated previously. The black sea bass (*Centropomus striata*) is a ubiquitous reef fish species found in the Gulf of Mexico and along the Atlantic coast of the United States, from Florida to the Gulf of Maine. This species is a target for important commercial and recreational fisheries along the Atlantic coast that are assessed by using statistical catch-at-age models (Musick and Mercer, 1977; NEFSC, 2020; ASMFC²). Adult black sea bass are most abundant in temperate shelf environments, although their young (<2 years in age) often occur in estuarine and coastal habitats. The aging method for black sea bass has been validated through marginal increment analysis (Dery and Mayo, 1988; Penttila and Dery, 1988; Robillard et al.³; Koob et al., 2021).

We hypothesized that cycles of microconstituent deposition (i.e., chemical zonation) would relate to age with a dominant periodicity of 1 cycle per optical annulus. By linking the optical interpretation to the chemical measures, the periodicity of each cycle can be tested through time-series analysis. We first identified candidate microconstituents through elemental profiles and 2-dimensional (2D) maps. We then conducted Lomb–Scargle periodogram analyses on candidate microconstituent profiles to test the hypothesis that the dominant periodicity is 1.0 cycle per optical annulus. Under the premise that black sea bass

undertake a habitat shift from inshore to offshore waters during their second year of life, 2 alternate periodogram analyses were conducted with data sets containing concentrations of microconstituents along a line from the core to the edge of otoliths for 1) the entire series of annuli on each otolith or 2) the series of annuli after the first one.

Materials and methods

Analysis of otoliths

Sagittal otoliths were collected from black sea bass (sample size $[n]=125$) ranging in total length from 19.5 to 36.3 cm and captured through hook and line at wreck and artificial reef sites (depths: 20–30 m) off Ocean City, Maryland, during the summer and fall of 2016 and 2018. Annuli in whole and sectioned otoliths were defined as continuous opaque zones with no breaks (Fig. 1). Aging conventions were adopted from Robillard et al.³ and Koob et al. (2021), who discounted initial opaque material deposited around the core of an otolith as material formed during age 0 and identified a second opaque region as the completion of the first annulus (Fig. 1) (Penttila and Dery, 1988; Robillard et al.³).

By convention, a birth date of 1 January was assumed (given that spawning occurs in the spring for this species) (Vanderkooy et al.⁴). The seasonality of optical and chemical annuli could vary; therefore, fish collected before 30 June were assumed to have completed less than half of their most recent year of life, and counts of opaque zones were assumed to represent the estimated age. For those captured after 30 June, the edge was counted as an integer because these fish had completed >0.5 years of life and so that we could consider the indication of growth patterns beyond the last opaque zone (Dery and Mayo, 1988; Vanderkooy et al.⁴). Whole otoliths from black sea bass were photographed under reflected light at 1.5× magnification by using a microscope camera and Infinity Analyze and Capture⁵ software (vers. 6.5.6; Teledyne Lumenera, Ottawa, Canada). Following age assignment with whole otoliths, otoliths were then embedded in Struers epoxy resin (Struers A/S, Ballerup, Denmark) for sectioning. A 2.0-mm-thick section containing the core region (the innermost portion of the otolith, pertaining to the first year of life) was cut along a transverse plane with an IsoMet Low Speed Saw (Beuhler Ltd., Lake Bluff, IL). The otolith section was then attached to a glass slide by using Crystalbond 509 mounting adhesive (Aremco Products Inc., Valley Cottage, NY) in preparation for microchemical analysis and further interpretations of annuli.

² ASMFC (Atlantic States Marine Fisheries Commission). 2021. Review of the interstate fishery management plan for black sea bass (*Centropomus striata*): 2020 fishing year, 15 p. ASMFC, Arlington, VA. [Available from [website](#).]

³ Robillard, E., J. W. Gregg, J. Dayton, and J. Gartland. 2016. Validation of black sea bass, *Centropomus striata*, ages using oxytetracycline marking and scale margin increments, 17 p. Stock Assess. Rev. Comm., SARC 62 working paper. [Available from Northeast Fish. Sci. Cent., Natl. Mar. Fish. Serv., NOAA, 166 Water St., Woods Hole, MA.]

⁴ Vanderkooy, S., J. Carroll, S. Elzey, J. Gilmore, and J. Kipp. 2020. A practical handbook for determining the ages of Gulf of Mexico and Atlantic coast fishes, 3rd ed., 268 p. Gulf States Mar. Fish. Comm., Ocean Springs, MS. [Available from [website](#).]

⁵ Mention of trade names or commercial companies is for identification purposes only and does not imply endorsement by the National Marine Fisheries Service, NOAA.

Microchemical analysis of elemental variations from the core region to the otolith's periphery was done by using laser ablation inductively coupled plasma mass spectrometry (LA-ICP-MS) at the Department of Geological Sciences of the University of Texas at Austin. Analysis was limited to 34 of the 125 otoliths collected because of the cost of the analysis; otoliths were randomly selected from among otoliths taken from fish assigned ages >1 year. The instrumentation used was an NWR193 excimer laser ablation system (193-nm wavelength, 4-ns pulse width; Elemental Scientific Inc., Omaha, NE) coupled to an Agilent 7500ce ICP-MS (Agilent, Santa Clara, CA). This LA-ICP-MS system was equipped with a large-format, 2-volume sample cell with fast washout (<1 s) that accommodated all samples and standards (USGS MACS-3, NIST 612, and ECRM-752-NP) in 3 laser cell loadings.

The LA-ICP-MS system was optimized daily for sensitivity across the atomic mass unit range and low oxide production (ratio of thorium monoxide to thorium: 0.58 [standard deviation (SD) 0.06]) by tuning with a standard glass (NIST 612), and sensitivity was checked with trial transects on representative specimens. Following pre-ablation (75- μm spot, 50- $\mu\text{m}/\text{s}$ scan rate, 3.3- J/cm^2 energy density [fluence]) to remove shallow surface contaminants, core-to-edge profiles were collected from each otolith along the sulcal ridge for consistency, by using a spot with a 50- μm diameter, a 5- $\mu\text{m}/\text{s}$ scan rate, a fluence of 2.92 J/cm^2 (SD 0.15), a 15-Hz repetition rate, and carrier gas flows of 0.8 L/min for argon and 0.80–0.85 L/min for helium. The quadrupole time-resolved method was used to measure 12 masses with integration times of 10 ms (^{24}Mg , $^{43-44}\text{Ca}$, and ^{88}Sr), 20 ms (^{25}Mg , ^{31}P , and ^{55}Mn), and 25 ms (^{59}Co , ^{63}Cu , ^{66}Zn , and $^{137-138}\text{Ba}$). The quadrupole duty cycle of 0.3732 s corresponds to 94% of total measurement time, with a resultant linear sampling rate of 1.867 $\mu\text{m}/\text{s}$, equivalent to 13.4 measurements captured within the footprint of either aperture. Measured intensities were converted to elemental concentrations (parts per million) by using *iolite 4* software (Paton et al., 2011), with ^{43}Ca as the internal standard and a Ca index weight percentage of 38.3% for unknowns.

For the otoliths, USGS MACS-3 (synthetic aragonite) was used as the primary calibration standard, and NIST 612 (glass) and ECRM-752-NP (nanoparticulate pressed limestone powder pellet made from BCS-CRM 393 limestone from Bureau of Analysed Samples Ltd., Middlesbrough, UK) were used as external reference standards. The grand average of secondary standard recovery fractions for all elements was typically within 5% of preferred values in the GeoReM database (Jochum et al., 2005).

To create 2D maps of otolith microconstituents, areas were scanned by using contiguous line traverses with a 17- μm^2 aperture, spaced 17 μm apart. The scan rate (105 $\mu\text{m}/\text{s}$) was set to provide 1 quadrupole measurement cycle per aperture footprint. Using the quadrupole method for mapping, we surveyed elements with integration times of 10 ms ($^{43-44}\text{Ca}$ and ^{88}Sr), 20 ms (^{55}Mn and ^{138}Ba), and 25 ms (^{24}Mg , ^{65}Cu , and ^{66}Zn) and with a significantly shorter duty cycle of 0.1612 s corresponding to 90% of total measurement time. Calibration and secondary standards were

as described previously. External reference standard recoveries were typically within 10% of certified reference values. Image conversions, from contiguous-line traverses along the otolith to 2D maps of element deposition, were performed by using *iolite 4* software (Paton et al., 2011).

Analysis of time series

To determine if optical annuli coincide with the microconstituent profiles, LA-ICP-MS data were aligned with micrographs of transverse otolith sections through image analysis. Optical annuli were assigned and measured for each cycle of a paired translucent zone and opaque zone. Distances along the trench formed through ablation on the surface of an otolith were measured from the ablated point within the core region to the distal edge of each opaque zone according to optical annulus assignments (Fig. 1C), with a minimum of 39 measurements per year of growth. Each opaque zone was considered the terminus of each annulus (1 year of growth), and zones measured through LA-ICP-MS within a cycle (pair of translucent and opaque zones) were converted to fractional ages within each annulus cycle, assuming that otolith growth was linear.

Typical concentrations of elements over transects on otoliths from representative specimens were 10–10,000 times higher than the limits of detection for most elements (Table 1). A rule-of-thumb ratio of signal to noise of 2 to 3 was employed as a threshold for inclusion (mean transect concentration divided by minimum detection limit) (Armbruster and Pry, 2008; Rajaković et al., 2012). Consecutive moving average filters were used to smooth derived elemental time series (profiles) by using a 9-point boxcar width (13- and 26- μm equivalent distances), and the profiles were converted to Z-scores, resulting in smooth, locally weighted signals that were free from high-frequency outliers. Signals were converted to distance (in microns) from the core on the basis of scan rate and duty cycle. Because signals for elements measured with

Table 1

Average concentrations (in parts per million) of elements in otoliths of black sea bass (*Centropristis striata*) ($n=34$) caught off Ocean City, Maryland, during the summer and fall of 2016 and 2018. Also provided for each element are the standard deviation (SD) of the average concentration and the ratio of signal to noise (S:N), which is the mean transect concentration divided by the estimated mean detection limit among the analyzed otoliths. The elements are magnesium (Mg), phosphorus (P), manganese (Mn), cobalt (Co), copper (Cu), zinc (Zn), strontium (Sr), and barium (Ba). An asterisk (*) indicates that the average concentration of the element was less than twice as high as detection limits.

Value	Mg	P	Mn	Co	Cu	Zn	Sr	Ba
Average	13.6	78.6	2.3	0.2	0.3	0.4	2148.9	10.1
SD	3.0	32.5	0.8	0.0	1.2	0.4	168.4	3.5
S:N	23.7	2.7	4.6	3.2	0.3*	0.3*	45,000.0	370.0

multiple isotopes were identical, we used the isotopes with the highest abundance (e.g., ^{24}Mg and ^{138}Ba) for plotting and statistical analysis. The detrended time series for each individual fish and element were subjected to Lomb–Scargle periodogram analysis, a flexible approach that accounts for unequally spaced measurements across the annuli of multiple otoliths (Lomb, 1976; Scargle, 1982; Ruf, 1999). Normalized power was used to evaluate significant frequencies. Alternate periodogram analyses were performed with data for the entire series of annuli on each otolith and with data for the series of annuli after the first one on each otolith.

Results

Analysis with mass spectrometry

The elements Mg, Mn, Co, Cu, Zn, Sr, and Ba were all measured at detectable levels though LA-ICP-MS (Table 1). Copper and Zn were below the signal, a noise threshold

of 2.0–3.0 (both at a signal-to-noise ratio of 0.3), and were not considered further in analyses. Concentration amplitudes were within the range expected for otoliths from marine teleost fish: <1 ppm for transition metals Mn, Co, Cu, and Zn; <8 ppm for Mg, P, and Ba; and <2000 ppm for Sr (Campana, 1999; Hüsey et al., 2021b).

Among measured elements, Mg had the sharpest contrast across presumed chemical annuli as revealed in 2D maps of element deposition for the 2 analyzed otoliths (Fig. 2). The chemical zonation for 4 of the 6 elements analyzed, Ba, Mg, Mn, and Sr, aligned with conventional light microscopy. For Ba, chemical zonation was most apparent for annuli after the second one, with weak contrast prior to the third annulus. Strong zonation of Mg was observed for the entire series of annuli. For Mn, concentrations were elevated in the core region for both scanned otoliths, and chemical zonation was faint but distinct across the series of annuli. Zonation of Sr was inconsistent between the 2 otoliths (Fig. 2, “Sr” panel in both sets of panels), with a faint series of annuli in one otolith and a narrow chemical zonation for annuli after the second one in the other otolith.

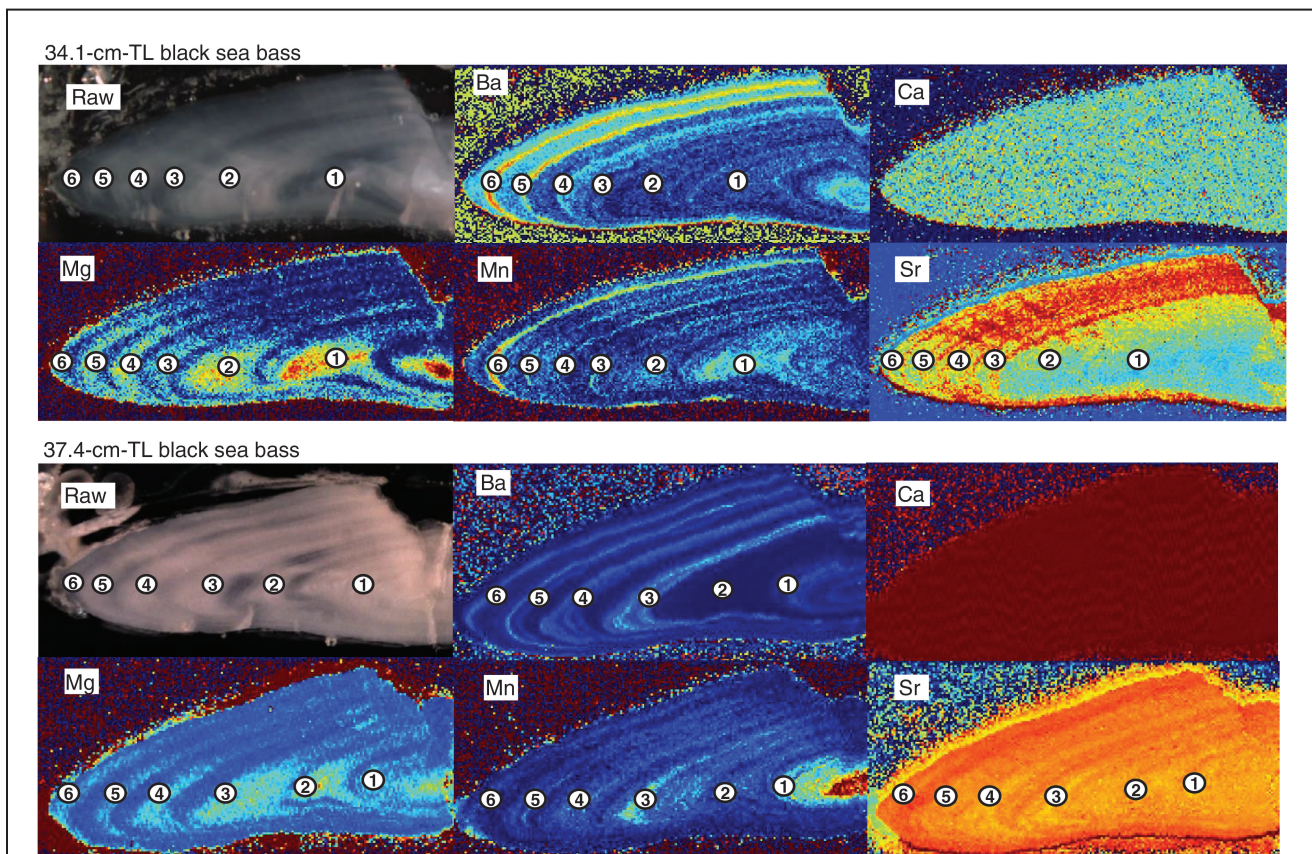


Figure 2

Two-dimensional maps of element deposition, with a light micrograph (Raw) image, for each of the sectioned otoliths from 2 black sea bass (*Centropristis striata*) caught on 15 July 2018 off Ocean City, Maryland. The elements are barium (Ba), calcium (Ca), magnesium (Mg), manganese (Mn), and strontium (Sr). Colors in the maps indicate the concentration of elements from blue (low) to red (high). Note that contrast is optimized and depicted through pseudocolor for each map, and it is not common across elements. White circles indicate optical annuli, and the associated numerals indicate assigned ages; the central opaque core is not included because it was not counted in otolith aging.

Zonation of Ca was homogeneous in both 2D maps as expected.

Despite notable zonation in the 2D maps, oscillating patterns in standardized elemental profiles were not aligned across individuals nor clearly associated with age (Fig. 3). Note that the majority of profiles correspond to estimated ages ≤ 4 years, with 2 profiles continuing to age 6. Profiles for the transition metal Co were especially noisy, corresponding to the lack of patterning in the 2D scan. For Ba, Mg, and Mn, peaks and nadirs of oscillations give some indication of association with optical annuli, but visual classifications were deemed too subjective.

Analysis with periodograms

The results of the principal periodogram analysis of the entire elemental time series, inclusive of the first annulus, indicate a significant periodicity in microchemical transects, albeit at frequencies that mostly differed from the expected 1 year (Fig. 4, top set of panels). Only annular deposition of Mg had significant periodicity of 1 cycle per annulus. Significant periodicity in deposition is evident for the elements Ba and Mn but at a rate of ~ 1.5 cycles per annulus, each at a lower normalized power

than that for deposition of Mg (Fig. 4, top set of panels). Strontium had no defined peak in oscillations and, therefore, no determinable primary chemical cycle. In the periodograms for oscillations of P and Co, the frequencies are 1.5 cycles and 1 cycle per annulus, respectively, albeit at low normalized power (i.e., reduced significance).

In the alternative periodogram analysis of the time series excluding the first annulus, significant periodicity was detected for oscillations of Mg, Ba, Mn, and P at the hypothesized 1 cycle per annulus at high normalized power (Fig. 4, bottom set of panels). Magnesium deposition periodicity remained at 1 cycle per annulus after truncation of the time series. The periodogram for oscillations of Sr again failed to indicate a dominant period. In the truncated series, oscillations of Co had multiple peaks, all of which deviated from the expected frequency of 1 year.

Discussion

The hypothesis of aligned optical and chemical oscillations across all annuli (not excluding the first annulus) was confirmed for the element Mg and alignment across age estimates >1 year was confirmed for the microconstituents

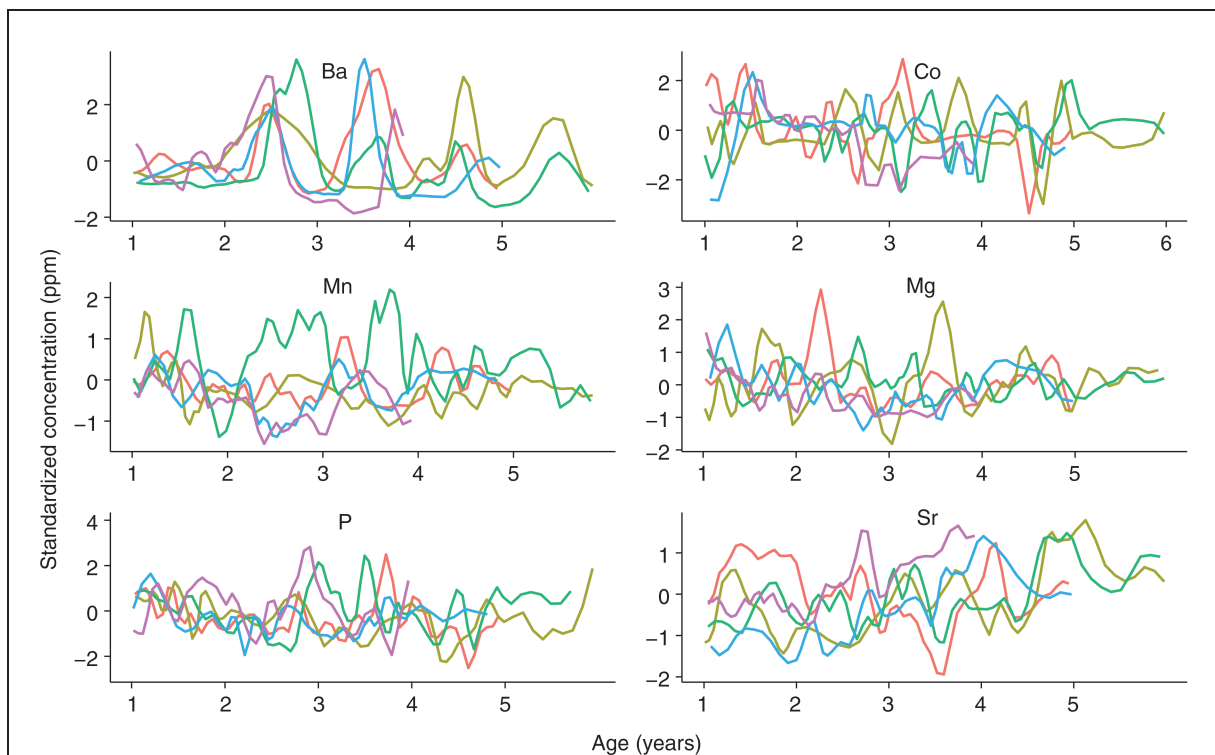
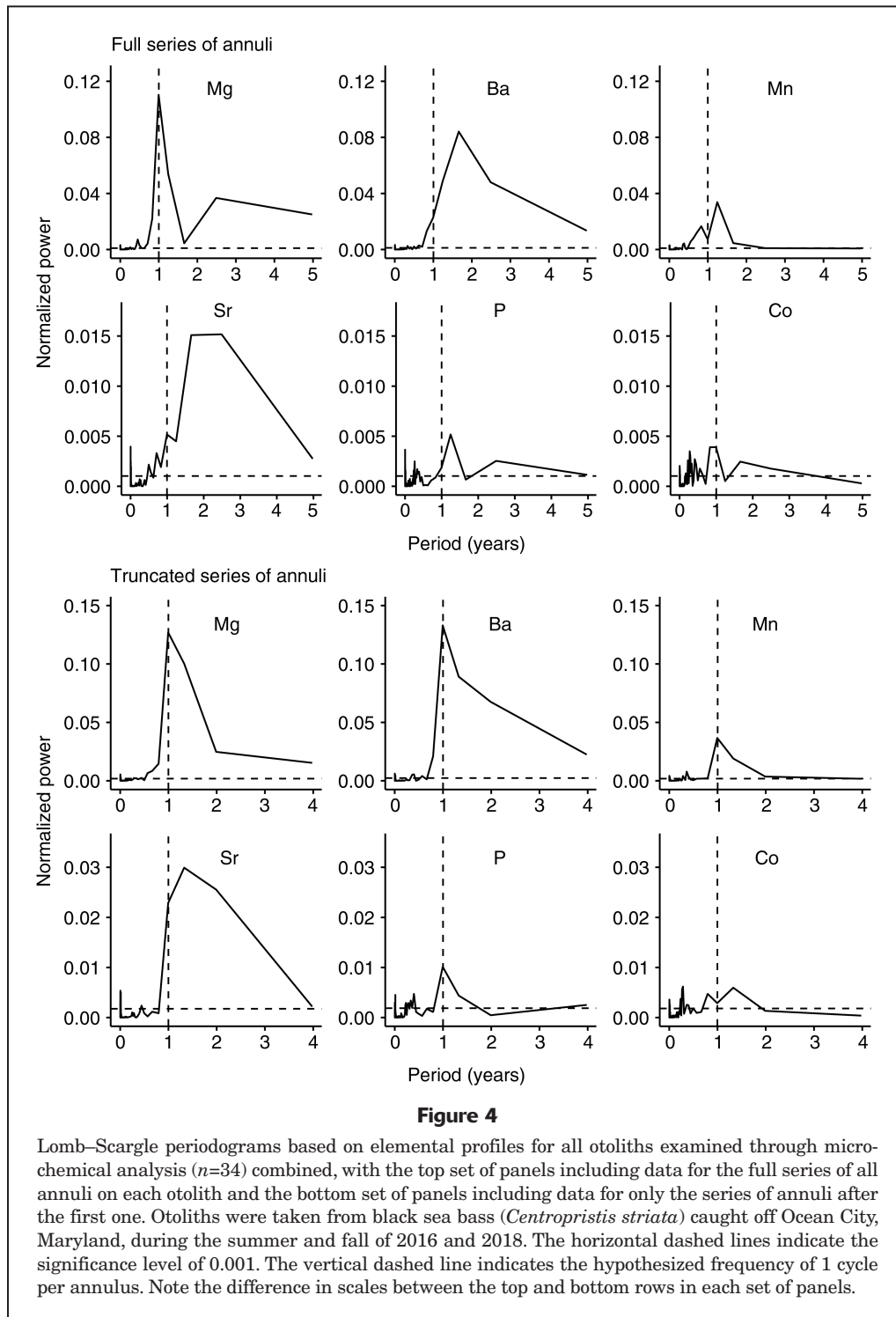


Figure 3

Profiles of microconstituent concentrations, smoothed by using consecutive moving median and average filters, in 5 of the 34 otoliths examined through laser ablation inductively coupled plasma mass spectrometry. Otoliths were taken from black sea bass (*Centropristis striata*) caught off Ocean City, Maryland, in October and July 2018. The microconstituents are barium (Ba), cobalt (Co), manganese (Mn), magnesium (Mg), phosphorus (P), and strontium (Sr). The lines for the individual otoliths are depicted in different colors for readability.



Ba, Mg, P, and Mn through the Lomb–Scargle periodogram analyses. The periodicity we observed for deposition of Mg in otoliths through the analysis that included data for all annuli supports recent work by Koob et al. (2021) and the conventions used by the Northeast Fisheries Science Center for first annulus assignments. Because the dominant period was 1 year, rather than for instance 1.2 years, the

influence of the assumption that otolith growth is linear on the estimated period was negligible. The 2D maps show that chemical zonation corresponded with optical zonation for all annuli in each otolith (in the case of Mg) or for the annuli after the first one in each otolith (in the cases of Ba, P, and Mn). Concentrations of other elements were below detection thresholds (Cu and Zn), had no zonation (Co), or

had patterns that were inconsistent with optical annuli (Sr). Patterns of Sr oscillations are weak in 2D maps and in standardized profiles. This lack of annual periodicity in Sr explains why X-ray dispersive spectroscopy of Sr deposition in otoliths was inconclusive in past work (Richards, 2016; Frey, 2022).

Both periodogram analysis results and 2D maps indicate a lack of consistent chemical zonation associated with the first optical annulus. The inclusion and removal of the first annulus in periodogram analysis had a large influence on the periodicity of Sr, Ba, and Mn oscillations. The shifts in Sr, Ba, and Mn concentrations could be explained by habitat changes occurring during the juvenile life stage. Nursery habitats in estuarine and nearshore environments for black sea bass (Dery and Mayo, 1988) are heterogeneous in ambient concentrations of Sr, Ba, and Mn. Strontium is conservatively mixed with and is often positively associated with salinity (Kraus and Secor, 2004), observations that are consistent with the lower otolith concentrations of Sr deposited during the first year of life than the levels deposited during later years in otoliths analyzed in our study (Fig. 2). Barium becomes less available in eutrophic waters of estuaries and coastal waters (Hüssy et al., 2021b), a finding that aligns with the lower otolith concentrations of Ba around the first optical annulus compared to the levels around the rest of the annuli beyond the first annulus in otoliths analyzed in our study. How Mn is associated with ambient exposure remains unsettled in the literature, although higher than normal concentrations of Mn in otoliths have been associated with hypoxic waters (Limburg and Casini, 2018). Early elemental oscillations could also reflect a change in reproductive state for black sea bass (maturation is achieved at ages ≥ 2 years) or early habitat transitions (Drohan et al., 2007). Understanding the lack of expected periodicity for age-1 black sea bass requires a deeper consideration of otolith composition during the first year of life.

Seasonal changes in otolith composition with regard to the elements Mg, Sr, and Mn have been found to conform to expectations of environmental and physiological influences (Grammer et al., 2017; Hüssy et al., 2021a). In their scheme, Hüssy et al. (2021a) proposed that otolith uptake of Ba, K, and Sr, versus that of P, Cu, and Zn, was respectively under environmental versus physiological controls. Further, Mg and Mn uptake was influenced jointly by the environment and physiology (Hüssy et al., 2021a). Concentration of Mg in otoliths is known to be linked to growth (Grammer et al., 2017), possibly explaining the strength of the periodogram analyses and the visibility of chemical annuli in the 2D maps created in our study. Results of recent work by Brophy et al. (2021) indicate that seasonal variation in deposition of Sr in otoliths is detectable in anglerfish (*Lophius piscatorius*), but in our analysis, Sr oscillations were weak and no yearly periodic fluctuations were apparent. Concentrations of Ba in otoliths, like those of Sr, may reflect seasonal temperature cycles (Barnes and Gillanders, 2013; Reis-Santos et al., 2013; Stanley et al., 2015).

A central premise of aligning otolith microconstituent cycles with annulus zone formation is that black sea bass

are exposed to seasonal changes in temperatures. Moser and Shepherd (2008) placed archival tags in black sea bass released off coastal states from Massachusetts to Virginia. These and conventionally tagged black sea bass made offshore migrations during winter months, cued by cooling temperatures in near-shelf regions. Off the coast of Maryland, black sea bass migrate to inner shelf regions in spring and reside in bottom waters that have stable thermal conditions until fall, when turnover or seasonal mixing causes a rapid increase in water column temperatures (Wiernicki et al., 2020). These conditions are then followed by cooling in late fall, cueing winter migrations of black sea bass to offshore waters (Moser and Shepherd, 2008). Off the coast of Maryland, where this study's samples originated, this pattern of residency in the spring and fall and offshore migration in winter would be associated with exposure to a seasonal amplitude in temperature of 12–17°C, with most of that change in temperature occurring during August–November (based on observed bottom temperatures in near- and mid-shelf waters off Delaware, Maryland, and Virginia; Rothermel et al. 2020). During a single, long-term (more than 3 years) mark-recapture study in which archival tags were used, Moser and Shepherd (2008) observed temperatures experienced by tagged fish that were consistent with this seasonal cycle and that ranged between 6°C (in winter) and 25°C (from late summer to fall). As reviewed in the “Introduction” section, seasonal temperature was expected to influence concentrations of Mg, Mn, Sr, and Ba—the elements that are incorporated into an otolith's aragonitic structure.

For temperate species, such as the black sea bass, changes in composition of an otolith are thought to relate to the formation of organic-rich (winter) and Ca-rich (spring, summer, and fall) zones in an otolith (Secor and Piccoli, 1996; Hüssy et al., 2021b). These optical zones are also associated with seasonal changes in temperature, with the translucent zone forming during high growth seasons of summer and fall and the narrow opaque zone forming during winter and early spring (Zlokovitz et al., 2003). For example, variation in the level of Sr in hard parts can serve as a proxy for oscillations in temperature: in cooler temperatures, higher levels of Sr are substituted for Ca in the lattice structure of a hard part (Engstedt et al., 2012). Such oscillations across the optical zones of otoliths have been observed for the temperate species red emperor (*Lutjanus sebae*) (Seyama et al., 1991) and bluefin tuna (*Thunnus thynnus*) (Siskey et al., 2016). Therefore, the variations in microchemical composition of otoliths across optical zones can validate the seasonal frequency of these chemical annuli.

Conclusions

In addition to their use in validation of microconstituent composition in otoliths, one could directly age individuals on the basis of chemical annuli rather than optical annuli. Such an approach would have application for species like the goosefish (*Lophius americanus*), for which optical

annuli are not easily interpreted (Bank et al., 2020). For black sea bass, optical annuli are well aligned with chemical annuli in the 2D maps created in our study (Fig. 2), especially those for Mg, indicating that age can be assigned through direct interpretation of the 2D maps of element deposition in otoliths. The high-contrast visualizations of such analysis of otoliths from black sea bass can provide improved precision in age validation for optical annuli interpretation (Limburg et al., 2018; Heimbrand et al., 2020; Hüsey et al., 2021b). On the other hand, for even moderate sample sizes ($n > 50$), reliance on 2D maps could be cost-prohibitive and demand greater investment in time than standard aging approaches. Further, 2D map interpretations are subjective and not supported by objective time-series analyses, such as the periodogram approach applied in our study.

Validation of direct aging through hard-part analysis provides the foundation for strong stock assessments. The results from our use of a chemical aging approach for black sea bass support the findings of recent marginal increment validation studies and optical annulus interpretations. Still, the variable interpretations of the first optical annulus in otoliths merit additional examination given the 1) varying results across the candidate elements Mg, Ba, P, and Mn and 2) past uncertainty in assignment of the first annulus. Chemical validation of optical annulus formation in otoliths of black sea bass further strengthens the confidence in accurate age data for age-structured black sea bass stock assessments.

Resumen

En este estudio, examinamos si los microconstituyentes de los otolitos se depositan estacionalmente de forma similar a la formación del anillo óptico y, por tanto, pueden utilizarse para validar las interpretaciones de la edad. En las especies templadas, los cambios estacionales de temperatura impulsan la formación de anillos ópticos, y suponemos que de la misma manera causan oscilaciones en la deposición de microconstituyentes. Utilizando análisis de espectrometría de masas con plasma de acoplamiento inductivo por ablación láser, comprobamos la periodicidad en la deposición de bario (Ba), calcio, cobre, magnesio (Mg), manganeso (Mn), fósforo (P), estroncio y zinc en los otolitos y comparamos esa periodicidad con la periodicidad de la zona anular (zonas ópticas opacas y translúcidas). Para esta investigación de la periodicidad de los anillos químicos, utilizamos serrano estriado (*Centropristis striata*), una especie para la que se ha validado la formación anual de anillos ópticos. Se detectaron periodicidades en los perfiles de los elementos de otolitos de lobina negra mediante análisis de periodogramas de Lomb-Scargle. La formación de anillos ópticos se alineó con los perfiles de Mg, pero la periodicidad en la deposición de anillos de otros elementos, Ba, Mn y P, se observó sólo después del primer anillo óptico, un resultado que es indicativo de los cambios ontogénicos en el hábitat (de aguas costeras a aguas cercanas a la plataforma) que se sabe ocurren durante la etapa

de vida juvenil de esta especie. Ciertos elementos, como el Mg, identificados mediante este análisis de otolitos y el análisis del periodograma podrían aplicarse a especies para las que no existe un procedimiento de validación de la edad.

Acknowledgments

This work was made possible by the NOAA Office of Education Educational Partnership Program (NOAA EPP) (award no. NA16SEC4810007) and through a NOAA EPP Living Marine Resources Cooperative Science Center Fellowship to the senior author.

Literature cited

- Armbruster, D. A., and T. Pry.
2008. Limit of blank, limit of detection and limit of quantitation. *Clin. Biochem. Rev.* 29:S49–S52.
- Arslan, Z., and D. H. Secor.
2005. Analysis of trace transition elements and heavy metals in fish otoliths as tracers of habitat use by American eels in the Hudson River estuary. *Estuaries* 28:382–393. [Crossref](#)
- Bank, C. M., K. Oliveira, S. J. Sutherland, M. P. Armstrong, J. Landa, and S. X. Cadrin.
2020. Age validation for goosefish (*Lophius americanus*) in the northeastern United States. *Fish. Bull.* 118:8–20. [Crossref](#)
- Barnes, T. C., and B. M. Gillanders.
2013. Combined effects of extrinsic and intrinsic factors on otolith chemistry: implications for environmental reconstructions. *Can. J. Fish. Aquat. Sci.* 70:1159–1166. [Crossref](#)
- Bradford, M. J.
1991. Effects of ageing errors on recruitment time series estimated from sequential population analysis. *Can. J. Fish. Aquat. Sci.* 48:555–558. [Crossref](#)
- Brophy, D., S. Pérez-Mayol, R. Duncan, K. Hüsey, A. J. Geffen, H. D. Gerritsen, M. C. Villanueva, and B. Morales-Nin.
2021. Elemental composition of illicia and otoliths and their potential application to age validation in white anglerfish (*Lophius piscatorius* linnaeus [sic], 1758). *Estuar. Coast. Shelf Sci.* 261:107557. [Crossref](#)
- Campana, S. E.
1997. Use of radiocarbon from nuclear fallout as a dated marker in the otoliths of haddock *Melanogrammus aeglefinus*. *Mar. Ecol. Prog. Ser.* 150:49–56. [Crossref](#)
1999. Chemistry and composition of fish otoliths: pathways, mechanisms and applications. *Mar. Ecol. Prog. Ser.* 188:263–297. [Crossref](#)
2001. Accuracy, precision and quality control in age determination, including a review of the use and abuse of age validation methods. *J. Fish Biol.* 59:197–242. [Crossref](#)
- Casselman, J. M.
1983. Age and growth assessment of fish from their calcified structures—techniques and tools. *In* Proceedings of the international workshop on age determination of oceanic pelagic fishes: tunas, billfishes, and sharks; Miami, 15–18 February 1982 (E. D. Prince and L. M. Pulos, eds.), p. 1–17. NOAA Tech. Rep. NMFS 8.
- Chale-Matsau, J. R., A. Govender, and L. E. Beckley.
2001. Age, growth and retrospective stock assessment of an economically extinct sparid fish, *Polysteganus undulosus*, from South Africa. *Fish. Res.* 51:87–92. [Crossref](#)

- Dery, L. M., and J. P. Mayo.
1988. Black sea bass, *Centropristis striata*. In Age determination methods for Northwest Atlantic species (J. Penttila and L. M. Dery, eds.), p. 59–69. NOAA Tech. Rep. NMFS 72.
- Drohan, A. F., J. P. Manderson, and D. B. Packer.
2007. Essential fish habitat source document: black sea bass, *Centropristis striata*, life history and habitat characteristics, 2nd ed. NOAA Tech. Memo. NMFS-NE-200, 68 p.
- Dwyer, K. S., S. J. Walsh, and S. E. Campana.
2003. Age determination, validation and growth of Grand Bank yellowtail flounder (*Limanda ferruginea*). ICES J. Mar. Sci. 60:1123–1138. [Crossref](#)
- Elvarsson, B. P., P. J. Woods, H. Björnsson, J. Lentin, and G. Thordarson.
2018. Pushing the limits of a data challenged stock: a size-and age-structured assessment of ling (*Molva molva*) in Icelandic waters using Gadget. Fish. Res. 207:95–109. [Crossref](#)
- Engstedt, O., P. Koch-Schmidt, and P. Larsson.
2012. Strontium (Sr) uptake from water and food in otoliths of juvenile pike (*Esox lucius* L.). J. Exp. Mar. Biol. Ecol. 418–419:69–74. [Crossref](#)
- Frey, B. A.
2022. Validation of age and growth using microconstituent analysis of fish hardparts. [sic] M.S. thesis, 89 p. Univ. Md., College Park, MD. [Available from [website](#).]
- Grammer, G. L., J. R. Morrongiello, C. Izzo, P. J. Hawthorne, J. F. Middleton, and B. M. Gillanders.
2017. Coupling biogeochemical tracers with fish growth reveals physiological and environmental controls on otolith chemistry. Ecol. Monogr. 87:487–507. [Crossref](#)
- Heimbrand, Y., K. E. Limburg, K. Hüsey, M. Casini, R. Sjöberg, A.-M. Palmén Bratt, S.-E. Levinsky, A. Karpushevskaia, K. Radtke, and J. Öhlund.
2020. Seeking the true time: exploring otolith chemistry as an age-determination tool. J. Fish Biol. 97:552–565. [Crossref](#)
- Hunt, J. J.
1980. Guidelines for age determination of silver hake, *Merluccius bilinearis*, using otoliths. J. Northwest Atl. Fish. Sci. 1:65–80.
- Hüsey, K., M. Krüger-Johnsen, T. B. Thomsen, B. D. Heredia, T. Næraa, K. E. Limburg, Y. Heimbrand, K. McQueen, S. Haase, U. Krumme et al.
2021. It's elemental, my dear Watson: validating seasonal patterns in otolith chemical chronologies. Can. J. Fish. Aquat. Sci. 78:551–566. [Crossref](#)
- Hüsey, K., K. E. Limburg, H. de Pontual, O. R. B. Thomas, P. K. Cook, Y. Heimbrand, M. Blass, and A. M. Sturrock.
2021. Trace element patterns in otoliths: the role of biomineralization. Rev. Fish. Sci. Aquac. 29:445–477. [Crossref](#)
- Jensen, A. C.
1970. Validation of ages determined from otoliths of Gulf of Maine cod. Trans. Am. Fish. Soc. 99:359–362. [Crossref](#)
- Jensen, A. C., and J. P. Wise.
1962. Determining age of young haddock from their scales. Fish. Bull. 61:439–450.
- Jochum, K. P., U. Nohl, K. Herwig, E. Lammel, B. Stoll, and A. W. Hoffman.
2005. GeoReM: a new geochemical database for reference materials and isotopic standards. Geostand. Geoanal. 29:333–338. [Crossref](#)
- Jolivet, A., J.-F. Bardeau, R. Fablet, Y.-M. Paulet, and H. de Pontual.
2008. Understanding otolith biomineralization processes: new insights into microscale spatial distribution of organic and mineral fractions from Raman microspectrometry. Anal. Bioanal. Chem. 392:551–560. [Crossref](#)
- Kohler, A. C.
1964. Variations in the growth of Atlantic cod (*Gadus morhua* L.). J. Fish. Board Can. 21:57–100. [Crossref](#)
- Koob, E. R., S. P. Elzey, J. W. Mandelman, and M. P. Armstrong.
2021. Age validation of the northern stock of black sea bass (*Centropristis striata*) in the Atlantic Ocean. Fish. Bull. 119:261–273. [Crossref](#)
- Kraus, R. T., and D. H. Secor.
2004. Incorporation of strontium into otoliths of an estuarine fish. J. Exp. Mar. Biol. Ecol. 302:85–106. [Crossref](#)
- Limburg, K. E., and M. Casini.
2018. Effect of marine hypoxia on Baltic Sea cod *Gadus morhua*: evidence from otolith chemical proxies. Front. Mar. Sci. 5:00482. [Crossref](#)
- Limburg, K. E., M. J. Wuenschel, K. Hüsey, Y. Heimbrand, and M. Samson.
2018. Making the otolith magnesium chemical calendar-clock tick: plausible mechanism and empirical evidence. Rev. Fish. Sci. Aquac. 26:479–493. [Crossref](#)
- Lomb, N. R.
1976. Least-squares frequency analysis of unequally spaced data. Astrophys. Space Sci. 39:447–462. [Crossref](#)
- Lux, F. E., and F. E. Nichy.
1969. Growth of yellowtail flounder, *Limanda ferruginea* (Storer), on three New England fishing grounds. Int. Comm. Northwest Atl. Fish., ICNAF Res. Bull. 6:5–25.
- Machias, A., N. Tsimenides, L. Kokokiris, and P. Divanach.
1998. Ring formation on otoliths and scales of *Pagrus pagrus*: a comparative study. J. Fish Biol. 52:350–361. [Crossref](#)
- Massmann, W. H.
1963. Annulus formation on the scales of weakfish, *Cynoscion regalis*, of Chesapeake Bay. Chesap. Sci. 4:54–56. [Crossref](#)
- Mayo, R. K.
1981. Age validation of redfish, *Sebastes marinus* (L.), from the Gulf of Maine-Georges Bank region. J. Northwest Atl. Fish. Sci. 2:13–19. [Crossref](#)
- Mills, K. H., and R. J. Beamish.
1980. Comparison of fin-ray and scale age determinations for lake whitefish (*Coregonus clupeaformis*) and their implications for estimates of growth and annual survival. Can. J. Fish. Aquat. Sci. 37:534–544. [Crossref](#)
- Morin, R., S. G. LeBlanc, and S. E. Campana.
2013. Bomb radiocarbon validates age and long-term growth declines in American plaice in the southern Gulf of St. Lawrence. Trans. Am. Fish. Soc. 142:458–470. [Crossref](#)
- Moser, J., and G. R. Shepherd.
2008. Seasonal distribution and movement of black sea bass (*Centropristis striata*) in the Northwest Atlantic as determined from a mark-recapture experiment. J. Northwest Atl. Fish. Sci. 40:17–28. [Crossref](#)
- Musick, J. A., and L. P. Mercer.
1977. Seasonal distribution of black sea bass, *Centropristis striata*, in the Mid-Atlantic Bight with comments on the ecology and fisheries of the species. Trans. Am. Fish. Soc. 106:12–25. [Crossref](#)
- NEFSC (Northeast Fisheries Science Center).
2020. Operational assessment of the black sea bass, scup, bluefish, and monkfish stocks, updated through 2018. Natl. Mar. Fish. Serv., Northeast Fish. Sci. Cent. Ref. Doc. 20–01, 160 p. [Available from [website](#).]
- Paton, C., J. Hellstrom, B. Paul, J. Woodhead, J., and J. Hergt.
2011. Ilolite: freeware for the visualisation and processing of mass spectrometric data. J. Anal. At. Spectrom. 26:2508–2518. [Crossref](#)

- Penttila, J., and L. M. Dery (eds.).
1988. Age determination methods for Northwest Atlantic species. NOAA Tech. Rep. NMFS 72, 132 p.
- Powles, P. M.
1966. Validity of ageing young American plaice from otoliths. Int. Comm. Northwest Atl. Fish., ICNAF Res. Bull. 3:103–105.
- Rajaković, L. V., D. D. Marković, V. N. Rajaković-Ognjanović, and D. Z. Antanasijević.
2012. Review: the approaches for estimation of limit of detection for ICP-MS trace analysis of arsenic. *Talanta* 102:79–87. [Crossref](#)
- Reis-Santos, P., S. E. Tanner, T. S. Elsdon, H. N. Cabral, and B. M. Gillanders.
2013. Effects of temperature, salinity and water composition on otolith elemental incorporation of *Dicentrarchus labrax*. *J. Exp. Mar. Biol. Ecol.* 446:245–252. [Crossref](#)
- Richards, R. A.
2016. 2016 monkfish operational assessment. Northeast Fish. Sci. Cent. Ref. Doc. 16–09, 109 p. [Available from [website](#).]
- Rothermel, E. R., M. T. Balazik, J. E. Best, M. W. Breece, D. A. Fox, B. I. Gahagan, D. E. Haulsee, A. L. Higgs, M. H. O'Brien, M. J. Oliver, et al.
2020. Comparative migration ecology of striped bass and Atlantic sturgeon in the US Southern mid-Atlantic bight [sic] flyway. *PLoS ONE* 15(6):e0234442. [Crossref](#)
- Ruf, T.
1999. The Lomb–Scargle periodogram in biological rhythm research: analysis of incomplete and unequally spaced time-series. *Biol. Rhythm Res.* 30:178–201. [Crossref](#)
- Scargle, J. D.
1982. Studies in astronomical time series analysis. II. Statistical aspects of spectral analysis of unevenly spaced data. *Astrophys. J.* 263:835–853. [Crossref](#)
- Secor, D. H., and P. M. Piccoli.
1996. Age- and sex-dependent migrations of striped bass in the Hudson River as determined by chemical microanalysis of otoliths. *Estuaries* 19:778–793. [Crossref](#)
- Seyama, H., J. S. Edmonds, M. J. Moran, Y. Shibata, M. Soma, and M. Morita.
1991. Periodicity in fish otolith Sr, Na, and K corresponds with visual banding. *Experientia* 47:1193–1196. [Crossref](#)
- Siskey, M. R., V. Lyubchich, D. Liang, P. M. Piccoli, and D. H. Secor.
2016. Periodicity of strontium: calcium across annuli further validates otolith-ageing for Atlantic bluefin tuna (*Thunnus thynnus*). *Fish. Res.* 177:13–17. [Crossref](#)
- Stanley, R. R. E., I. R. Bradbury, C. DiBacco, P. V. R. Snelgrove, S. R. Thorrold, and S. S. Killen.
2015. Environmentally mediated trends in otolith composition of juvenile Atlantic cod (*Gadus morhua*). *ICES J. Mar. Sci.* 72:2350–2363. [Crossref](#)
- Thomas, R. M.
1983. Back-calculation and time of hyaline ring formation in the otoliths of the pilchard off South West Africa. *South Afr. J. Mar. Sci.* 1:3–18. [Crossref](#)
- Vitale, F., L. A. Worsøe Clausen, and G. N. Chonchúir.
2019. Handbook of fish age estimation protocols and validation methods. ICES Coop. Res. Rep. 346, 180 p. [Available from [website](#).]
- Watson, J. E.
1964. Determining the age of young herring from their otoliths. *Trans. Am. Fish. Soc.* 93:11–20. [Crossref](#)
- Wiernicki, C. J., M. H. O'Brien, F. Zhang, V. Lyubchich, M. Li, and D. H. Secor.
2020. The recurring impact of storm disturbance on black sea bass (*Centropristis striata*) movement behaviors in the Mid-Atlantic Bight. *PLoS ONE* 15(12):e0239919. [Crossref](#)
- Wilhelm, M. R., M. D. Durholtz, and C. H. Kirchner.
2008. The effects of ageing biases on stock assessment and management advice: a case study on Namibian horse mackerel. *Afr. J. Mar. Sci.* 30:255–261. [Crossref](#)
- Yule, D. L., J. D. Stockwell, J. A. Black, K. I. Cullis, G. A. Cholwek, and J. T. Myers.
2008. How systematic age underestimation can impede understanding of fish population dynamics: lessons learned from a Lake Superior cisco stock. *Trans. Am. Fish. Soc.* 137:481–495. [Crossref](#)
- Zlokovitz, E. R., D. H. Secor, and P. M. Piccoli.
2003. Patterns of migration in Hudson River striped bass as determined by otolith microchemistry. *Fish. Res.* 63:245–259. [Crossref](#)